Thickness-dependent pinning in a superconductor thin film

D. Agassi[a)]
Naval Surface Warfare Center, Carderock Division, Bethesda, Maryland 20817

D. K. Christen and S. J. Pennycook
Oak Ridge National Laboratory, Oak Ridge, Tennessee 37831

(Received 2 March 2006; accepted 26 September 2006; published online 29 January 2007)

The dependence of critical current density j_c on film thickness (d) is calculated for the simple configuration of a semi-infinite finite-thickness superconductor film and a single vortex. This film-thickness dependence reflects the impact of vortex broadening in a thin film on its pinning by the film's edge or an internal surface. The calculated film-thickness variation of j_c in the range $d/\lambda < 2$, where λ denotes the penetration depth, is found to be proportional to $d^{-1/2}$. A parameter-free estimate of the ensuing critical current is within a factor of 3 of observed values in $YBa_2Cu_3O_7$ coated conductors. It is argued that this type of film-thickness scaling applies beyond the simple configuration considered here. © *2007 American Institute of Physics*.
[DOI: 10.1063/1.2399898]

I. INTRODUCTION

The current carrying capacity of thick $YBa_2Cu_3O_7$ (YBCO) films came recently into focus in the context of coated conductors (CCs), where success in increasing the current carrying capacity is crucial for high temperature superconductor technology.[1] Recent CC data of YBCO films, which were grown by different methods, indicate a critical current density which scales with film thickness d as $d^{-1/2}$ (Ref. 2) or $\exp(-d/d_0)$.[3,4] Epitaxial films exhibit the same type of critical current density thickness dependence.[4] This characteristic film-thickness dependence has been attributed to several factors. One suggestion is that it reflects the effect of surface-attached dislocations, which thread throughout the entire film thickness for sufficiently thin films, and then gradually heal with increasing thickness.[3] Another suggestion invokes pinning by point defects coupled with a crossover from a two-dimensional (2d) to three-dimensional (3d) pinning pattern with increase in the film thickness.[5] Other factors such as crystallographic misaligned YBCO (Ref. 3) and the elasticity of vortices over short distances[6] have also been suggested. Obviously, identification of the origin (or origins) of this characteristic critical current scaling law, whether it reflects a materials science issue or other physical properties, is critical for the success of future efforts. In this work we consider another possible source for the observed critical current thickness dependence which is associated with vortex broadening in a thin superconductor film.[7] This broadening is evidenced by the known vortex structures in the following two opposite limits. In the limit of very thin films, when $d \ll \lambda$ and λ denotes the penetration depth, at large distances ($\rho \gg \lambda^2/d$) from the vortex core the vortex field decays as ρ^{-3}, i.e., it is of an infinite extent.[8] This is the Pearl vortex. In the opposite limit of a very thick film, when $d \gg \lambda$, the vortex field decays exponentially over a distance λ from its core. This is the textbook Abrikosov vortex.[9] The drastic variation in vortex broadening with film thickness between the above two film-thickness limits has implications on its pinning properties. In this work we examine these implications for the simple configuration of a semi-infinite thin film. This particular configuration may provide a model for the situation in thin porous YBCO films grown on vicinal substrates, where the pores are larger than the penetration depth,[10] and may offer insights in the context of more realistic configurations in thin films and CC.

In weak magnetic fields, the connection between the vortex broadening and the critical current density is premised on the assertion that the critical current density is determined by pinning (attraction) of an individual vortex to the pertinent type of defects. Qualitatively, pinning by a defect is a result of partial leakage of the vortex magnetic field from the superconductor into the defect's nonsuperconducting volume, thereby lowering the energy cost of sustaining the vortex structure. This argument implies, in particular, that superconductor surfaces act as pinning sites, and the larger the spatial overlap of the (undistorted) vortex field (with respect to an Abrikosov vortex) and the defect volume, the stronger is the resulting pinning. Hence, the superconductor surfaces may serve as simple test cases for film-thickness scaling of vortex pinning. For CC, in particular, the pertinent defects may be low-angle grain boundaries.[11]

To explore this argument quantitatively in this work we consider pinning in the configuration of a semi-infinite thin film and a single vortex aligned parallel to its edge. The pertaining boundary conditions at the film's edge mandate addition of a fictitious image vortex, i.e., a vortex of opposite chirality at the mirror-reflected location of the source vortex.[12] That image vortex has the effect of attracting and spreading the source vortex field distribution closer to and along the edge.[9,13] This is analogous to situations in electrostatics, where the effect of an image charge mandated by the pertinent boundary conditions is to attract and spread the charge distribution of a source charge placed on a finite con-

[a)]Electronic mail: yehoshua.agassi@navy.mil

 © 2007 American Institute of Physics

Downloaded 18 Aug 2008 to 160.91.172.37. Redistribution subject to AIP license or copyright; see http://jap.aip.org/jap/copyright.jsp

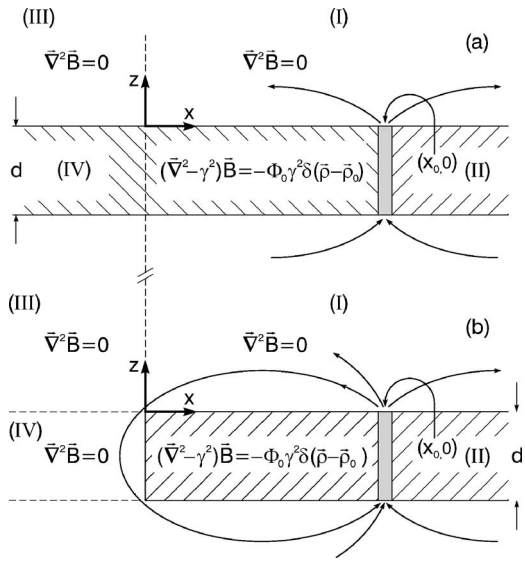

FIG. 1. The chosen coordinate system, the designation of space domains, and the associated defining field equations and definitions of the film thickness d and vortex location x_0 for an infinite and semi-infinite superconductor films. The superconductor body is denoted by the hatched area, and the shaft along the single vortex core is the gray strip at $(x_0,0)$. (a) denotes the infinite film, while (b) denotes the semi-infinite film.

ductor. Now, as the film thickness decreases the vortex field distribution broadens, thereby enhancing its field leakage out of the superconducting film. This field leakage enhancement is manifested by an increase in the pinning force with decreasing d. This qualitative argument implies a critical current enhancement for other types of extended defects such as large pores in the superconductor, twin boundaries and grain boundaries, which raises the question whether the corresponding critical current film-thickness dependence bears any resemblance to that observed in real systems.[1–4,10] As shown below, for the simple configuration analyzed here the answer is affirmative, see Eq. (23) and Fig. 4(b). If confirmed, this assertion implies that at least part of the observed $d^{-1/2}$ critical current scaling has an intrinsic origin.

The paper is organized as follows. In Sec. II we introduce the exact solution of a single vortex in a semi-infinite finite-thickness film. The last section contains the corresponding free energy and critical current calculations and a discussion of the results. Additional mathematical details are given in the Appendix.

II. VORTEX STRUCTURE IN A SEMI-INFINITE FINITE-THICKNESS FILM

The fields and currents associated with the configuration of a superconductor strip, a field, a vortex and combinations thereof have been treated before using various approaches.[13,14] The approach by Brandt[14] is general. However, to obtain the fields requires solving an integral equation numerically. For our purposes, however, i.e., the modeling of an empirical simple thickness scaling in terms of a simplified model, the alternative approach of Ref. 13 seems more transparent and hence it is adopted in the following.

As is evident already in the context of Fig. 1(a), and moreso in the context of Fig. 1(b) below, the fields in the different space domains are subject to different boundary conditions. To indicate their association with a particular space domain, all fields carry a self-explanatory superscript. In addition, some of the analytic *ansatze* in these space domains are constructed from the fields pertaining to a vortex in an infinitely extended film, Eq. (1). These "bare" fields carry an additional parenthetical superscript (V) to indicate their origin. All quantities are expressed in the cgs unit system.

In preparation for the calculations below, consider the structure of a single vortex in a finite-thickness film, Fig. 1(a),[13] i.e., the vortex fields *ansatz*

$$B_{x,y,z}^{(\mathrm{V})\mathrm{I+III}}(\mathbf{r};x_0) = \int_{-\infty}^{\infty} dk_x \int_{-\infty}^{\infty} dk_y e^{i(k_x x + k_y y) - \sqrt{k_x^2 + k_y^2} z} \times \alpha_{x,y,z}^{(\mathrm{V})\mathrm{I+III}}(x_0),$$

$$B_{x,y}^{(\mathrm{V})\mathrm{II+IV}}(\mathbf{r};x_0) = \int_{-\infty}^{\infty} dk_x \int_{-\infty}^{\infty} dk_y e^{i(k_x x + k_y y)} \times \frac{\sinh[D(k_x,k_y)(z+d/2)]}{\sinh[D(k_x,k_y)(d/2)]} \alpha_{x,y}^{(\mathrm{V})\mathrm{II+IV}}(x_0),$$

$$B_z^{(\mathrm{V})\mathrm{II+IV}}(\mathbf{r};x_0) = \int_{-\infty}^{\infty} dk_x \int_{-\infty}^{\infty} dk_y e^{i(k_x x + k_y y)} \times \frac{\cosh[D(k_x,k_y)(z+d/2)]}{\cosh[D(k_x,k_y)(d/2)]} \alpha_z^{(\mathrm{V})\mathrm{II+IV}}(x_0) + \left(\frac{\Phi_0 \gamma^2}{4\pi^2}\right) \int_{-\infty}^{\infty} dk_x \int_{-\infty}^{\infty} dk_y e^{i[k_x(x-x_0)+k_y y]} \times \frac{1}{D(k_x,k_y)^2},$$

$$D(k_x,k_y) = \sqrt{k_x^2 + k_y^2 + \gamma^2}, \quad \gamma = 1/\lambda. \tag{1}$$

The coordinate system employed in Eq. (1) and the domains in space are defined in Fig. 1(a), x_0 is the vortex core location, $\Phi_0 = \pi\hbar c/|e|$ is the magnetic flux quantum, and the second term in $B_z^{(\mathrm{V})\mathrm{II+IV}}$ corresponds to the source vortex with a core aligned along the z axis. Expressions (1) automatically satisfies the defining equations

$$\nabla^2 \mathbf{B}^{\mathrm{I+III}} = 0, \quad (\nabla^2 - \gamma^2)\mathbf{B}^{\mathrm{II+IV}} = -\Phi_0 \gamma^2 \delta(\boldsymbol{\rho} - \boldsymbol{\rho}_0), \quad \boldsymbol{\rho} = (x,y), \quad \boldsymbol{\rho}_0 = (x_0,0), \tag{2}$$

and the proper symmetry properties under the transformation $z \to -z-d$. The second equation in Eq. (2) is the London equation in superconductor domain. The fields in the portion of space where $z < -d$ follow from Eq. (1) by the replacement $z \to -z-d$.

Downloaded 18 Aug 2008 to 160.91.172.37. Redistribution subject to AIP license or copyright; see http://jap.aip.org/jap/copyright.jsp

The six α coefficients in Eq. (1) are determined by imposing the pertaining boundary conditions. Several equivalent sets may be used. One such set consists of three field continuity equations across the $z=0$ boundary, the two Maxwell equations $\nabla\cdot\mathbf{B}^{\mathrm{I+III}}=\nabla\cdot\mathbf{B}^{\mathrm{II+IV}}=0$, and the condition that the z-directed current at the $z=0$ boundary vanishes, i.e.,

$$\left(\frac{4\pi}{c}\right)j_z\bigg|_{z=0}=\frac{\partial B_y^{\mathrm{II+IV}}}{\partial x}-\frac{\partial B_x^{\mathrm{II+IV}}}{\partial y}\bigg|_{z=0}=0. \tag{3}$$

Solving the ensuing six linear equations yields the explicit expression

$$\begin{aligned}
\alpha_x^{(\mathrm{V})\mathrm{I+III}}(x_0)&=\alpha_x^{(\mathrm{V})\mathrm{II+IV}}(x_0)=-ik_xW(k_x,k_y)e^{-ik_xx_0},\\
\alpha_y^{(\mathrm{V})\mathrm{I+III}}(x_0)&=\alpha_y^{(\mathrm{V})\mathrm{II+IV}}(x_0)=-ik_yW(k_x,k_y)e^{-ik_xx_0},\\
\alpha_z^{(\mathrm{V})\mathrm{I+III}}(x_0)&=\sqrt{k_x^2+k_y^2}W(k_x,k_y)e^{-ik_xx_0},\\
\alpha_z^{(\mathrm{V})\mathrm{II+IV}}(x_0)&=-\frac{(k_x^2+k_y^2)W(k_x,k_y)e^{-ik_xx_0}}{D(k_x,k_y)\tanh[D(k_x,k_y)(d/2)]},\\
W(k_x,k_y)&=\frac{\gamma^2\Phi_0\tanh[D(k_x,k_y)(d/2)]}{4\pi^2\sqrt{k_x^2+k_y^2}D(k_x,k_y)\{\sqrt{k_x^2+k_y^2}+D(k_x,k_y)\tanh[D(k_x,k_y)(d/2)]\}}.
\end{aligned} \tag{4}$$

The advantage of expressions (1) and (4) in the Cartesian coordinates system over equivalent expressions in the cylindrical coordinates system[13] is their convenience in the context of a semi-infinite film.

Expressions (1) and (4) incorporate the Abrikosov-vortex structure distortion due to the finite film thickness. To account for the additional distortion due to the presence of an edge to the film it is necessary to consider the four spatial domains in Fig. 1(b). The defining equations in these domains are extensions of Eqs. (2), i.e.,

$$\nabla^2\mathbf{B}^{\mathrm{I,III,IV}}=0,\quad (\nabla^2-\gamma^2)\mathbf{B}^{\mathrm{II}}=-\Phi_0\gamma^2\delta(\boldsymbol{\rho}-\boldsymbol{\rho}_0). \tag{5}$$

The fields in the portion of space where $z<-d$ are the same as those in Fig. 1(a).

Consider first the solution in domain II in the form of vortex and antivortex pairs,[13] i.e.,

$$\mathbf{B}^{\mathrm{II}}(\mathbf{r};x_0)=\mathbf{B}^{(\mathrm{V})\mathrm{II+IV}}(\mathbf{r};x_0)-\mathbf{B}^{(\mathrm{V})\mathrm{II+IV}}(\mathbf{r};-x_0), \tag{6}$$

where $\mathbf{B}^{(\mathrm{V})\mathrm{II+IV}}(\mathbf{r};x_0)$ is given by Eqs. (1) and (4). The *ansatz* (6) obviously satisfies the London equation in (5), the zero-current boundary condition (3), and, by construction, its counterpart on the $x=0$ edge, i.e.,

$$\left(\frac{4\pi}{c}\right)j_x\bigg|_{x=0}=\frac{\partial B_z^{\mathrm{II}}}{\partial y}-\frac{\partial B_y^{\mathrm{II}}}{\partial z}\bigg|_{x=0}=0. \tag{7}$$

Thus, the *ansatz* (6) is the exact solution in domain II. The corresponding explicit expressions are quoted in the Appendix.

We now proceed to consider the field in domain IV, Fig. 1(b). The corresponding expressions are constructed as follows. The continuity of B_x across the $x=0$ surface, the defining equation $\nabla^2\mathbf{B}^{\mathrm{IV}}=0$, and the expected symmetry properties under the transformation $z\to-z-d$ are sufficient to determine the structure of the expression of $B_x^{(\mathrm{IV})}(\mathbf{r})$. From the integration of the Maxwell equation $\nabla\times\mathbf{B}^{\mathrm{IV}}=0$ in domain IV, specifically the conditions $j_z^{\mathrm{IV}}=j_y^{\mathrm{IV}}=0$, the structure of the $B_y^{(\mathrm{IV})}(\mathbf{r})$ and $B_z^{(\mathrm{IV})}(\mathbf{r})$ is obtained. Finally, taking the real parts of these expressions and matching them with the fields expressions in Eq. (6) at $x=0$ yields

$$\begin{aligned}
B_x^{\mathrm{IV}}(\mathbf{r};x_0)&=\int_0^\infty dk_x\int_0^\infty dk_y\cos(x\sqrt{k_x^2+\gamma^2})\cos(k_yy)\\
&\quad\times\frac{\sinh[D(k_x,k_y)(z+d/2)]}{\sinh[D(k_x,k_y)(d/2)]}\alpha_x^{\mathrm{IV}}(x_0),\\
B_y^{\mathrm{IV}}(\mathbf{r};x_0)&=\int_0^\infty dk_x\int_0^\infty dk_y\sin(x\sqrt{k_x^2+\gamma^2})\sin(k_yy)\\
&\quad\times\frac{\sinh[D(k_x,k_y)(z+d/2)]}{\sinh[D(k_x,k_y)(d/2)]}\alpha_y^{\mathrm{IV}}(x_0),\\
B_z^{\mathrm{IV}}(\mathbf{r};x_0)&=\int_0^\infty dk_x\int_0^\infty dk_y\sin(x\sqrt{k_x^2+\gamma^2})\cos(k_yy)\\
&\quad\times\frac{\cosh[D(k_x,k_y)(z+d/2)]}{\cosh[D(k_x,k_y)(d/2)]}\alpha_z^{\mathrm{IV}}(x_0),
\end{aligned} \tag{8}$$

where

$$\alpha_x^{\mathrm{IV}}(x_0)=-8k_xW(k_x,k_y)\sin(k_xx_0),$$

$$\alpha_y^{\mathrm{IV}}(x_0)=\frac{8k_xk_yW(k_x,k_y)\sin(k_xx_0)}{\sqrt{k_x^2+k_y^2}},$$

Downloaded 18 Aug 2008 to 160.91.172.37. Redistribution subject to AIP license or copyright; see http://jap.aip.org/jap/copyright.jsp

$$\alpha_z^{\mathrm{IV}}(x_0) = -\frac{8k_x W(k_x,k_y)D(k_x,k_y)\sin(k_x x_0)}{\sqrt{k_x^2+k_y^2}\tanh[D(k_x,k_y)(d/2)]}. \tag{9}$$

Expressions (8) and (9) constitute the exact field solution in domain IV. By construction they satisfy the field continuity boundary conditions at the interface $x=0$, the Maxwell equations $\nabla\times\mathbf{B}^{\mathrm{IV}}=0$ and $\nabla\cdot\mathbf{B}^{\mathrm{IV}}=0$, and consequently the Laplace equation $\nabla^2\mathbf{B}^{\mathrm{IV}}=0$ in Eq. (5). Equations (8) and (9) together with Eqs. (1) and (4) constitute the exact field solutions over the entire infinite spatial slab $0\geqslant z\geqslant -d$.

The exact solutions in domains II and IV, Fig. 1(b), can be continued to the rest of space by means of the Green theorem. A suitable Green function $G(\mathbf{r};\mathbf{r}_0)$ pertaining to the Laplace equation in domains I and III, which vanishes at $|z|\to\infty$, is the textbook result[15]

$$G(\mathbf{r};\mathbf{r}_0) = G(\mathbf{r}-\mathbf{r}_0) = -\frac{1}{4\pi|\mathbf{r}-\mathbf{r}_0|}, \tag{10}$$

which satisfies

$$\nabla^2 G(\mathbf{r};\mathbf{r}_0) = \delta(\mathbf{r}-\mathbf{r}_0). \tag{11}$$

It follows from the Green theorem and the exact solution in domains II and IV that the exact solution in domains I and III is

$$\mathbf{B}^{\mathrm{I,III}}(\mathbf{r};x_0) = \int_{-\infty}^{\infty}\int_{-\infty}^{\infty} dx'dy' G(\mathbf{r}-\mathbf{r}')\mathbf{B}^{\mathrm{II+IV}}[\mathbf{r}' = (x',y',z'=0);x_0]. \tag{12}$$

As can be easily established, expression (12) satisfies the defining equation $\nabla^2\mathbf{B}^{\mathrm{I,III}}=0$. It also satisfies the Maxwell equations $\nabla\cdot\mathbf{B}^{\mathrm{I,III}}=0$ and $\nabla\times\mathbf{B}^{\mathrm{I,III}}=(4\pi/c)\mathbf{j}^{\mathrm{I,III}}=0$. The latter follow from noting that $\nabla_{\mathbf{r}}G(\mathbf{r}-\mathbf{r}')=-\nabla_{\mathbf{r}'}G(\mathbf{r}-\mathbf{r}')$, integrating (12) by parts, and also the Green function, the $\mathbf{B}$, and all field derivatives in domains II and IV vanish at infinity. Thus the field expressions (12) indeed constitute the exact solution in the I and III portions of space.

III. THE CRITICAL CURRENT AND DISCUSSION

Following the methodology employed in electrostatics, where the electrostatic potential as function of the spatial coordinates is the potential energy of a probe charge at that point, the pinning potential is obtained below by calculating the free energy of a probe vortex as function of its location.[11,16] In the limit of a homogeneous, infinite-volume sample and a single Abrikosov vortex, the corresponding free energy is a constant. By contrast, in the configuration of a semi-infinite finite-thickness film with a single vortex aligned parallel to its edge, the film's edge introduces a gradient in the vortex free energy. This gradient determines the force that attracts the vortex toward that edge and the associated critical current.

The free energy F of an isotropic superconductor in the absence of an external field is given by[9,12,17]

$$F = \frac{1}{8\pi}\int_v dv[\mathbf{B}\cdot\mathbf{B} + \lambda^2(\nabla\times\mathbf{B})\cdot(\nabla\times\mathbf{B})]. \tag{13}$$

The integration in Eq. (13) is over all space v, *except* for the shaft in the superconductor along the vortex core, see Fig. 1. That shaft is commonly introduced to extricate the mathematical infinity associated with the singular (δ function) representation of the vortex core in the London equation, e.g., Eq. (5). The $\mathbf{B}\cdot\mathbf{B}$ term in Eq. (13) represents the potential energy stored in the magnetic field, while the second term represents the kinetic energy associated with the screening currents confined to the superconductor volume. By invoking the identity $(\nabla\times\mathbf{B})\cdot(\nabla\times\mathbf{B})=\nabla\cdot[\mathbf{B}\times(\nabla\times\mathbf{B})] - \mathbf{B}\cdot\nabla^2\mathbf{B}$, employing the London equation (5), and dividing the volume integration between that pertaining to the outside and inside the superconductor volume and the Gauss's theorem,[18] the expression for the free energy Eq. (13) takes the equivalent form,

$$F = \frac{1}{8\pi}\int_{\mathrm{out}} dv\mathbf{B}\cdot\mathbf{B} + \frac{\lambda^2}{8\pi}\int_S d\mathbf{s}\cdot[\mathbf{B}\times(\nabla\times\mathbf{B})] = F^{(\mathrm{out})} + F^{(\mathrm{surf})}. \tag{14}$$

In Eq. (14), the "out" superscript indicates integration over the volume outside the superconductor film, while the "surf" superscript indicates integration over the superconductor film surface S, *including* that of the shaft along the vortex core. The vector $d\mathbf{s}$ points outward the superconductor volume.[15] For notational simplicity, the dependence of F in Eq. (14) and of some of the subsequent expressions below on the vortex location x_0 and film thickness d is suppressed until the point in the discussion where these dependencies becomes relevant.

The first term $F^{(\mathrm{out})}$ term in Eq. (14) is approximated by the expression

$$F^{(\mathrm{out})} \approx \frac{1}{8\pi}\int_{-\infty}^{0}dx\int_{-\infty}^{\infty}dy\int_{-d}^{0}dz\mathbf{B}^{\mathrm{IV}}\cdot\mathbf{B}^{\mathrm{IV}} + \frac{1}{4\pi}\int_{-\infty}^{\infty}dx\int_{-\infty}^{\infty}dy\int_{0}^{\infty}dz\mathbf{B}^{(\mathrm{V-AV})\mathrm{I+III}}\cdot\mathbf{B}^{(\mathrm{V-AV})\mathrm{I+III}}. \tag{15}$$

The first term in Eq. (15) involves the exact field expressions in domain IV of space, Eqs. (2), (8), and (9). With regard to domains I and III, the exact field expressions are given by Eq. (12). The latter, however, is cumbersome to use in the free energy calculations. It is for this reason why for the field in domains I and III [Fig. 1(b)], we adopt the approximate expressions of the vortex and antivortex pair *ansatz* [Eq. (6) and Appendix], however, extended to domains I and III. These field is denoted by $\mathbf{B}^{(\mathrm{V-AV})\mathrm{I+III}}$ in Eq. (15), alluding to it expression in Eq. (6). By construction, the $\mathbf{B}^{(\mathrm{V-AV})\mathrm{I+III}}$ is continuous with the $\mathbf{B}^{\mathrm{II}}$, which is exact in domain II [Fig. 1(b)]. Therefore it is expected that $\mathbf{B}^{(\mathrm{V-AV})\mathrm{I+III}}$ provides a good approximation in domains I and III, at least in the immediate proximity to the $z=0$ surface of domain I wherefrom most of the contribution to the second term of Eq. (15) originates.

The second term in the free energy expression [Eq. (14)] is simplified as follows. Applying integration by parts, noting that all fields and their derivatives vanish at infinity and that $\nabla\cdot\mathbf{B}^{\mathrm{II}}=0$, yields

Downloaded 18 Aug 2008 to 160.91.172.37. Redistribution subject to AIP license or copyright; see http://jap.aip.org/jap/copyright.jsp

$$F^{(\mathrm{surf})} = \frac{\lambda^2}{8\pi}\left[2\int_0^\infty dx\int_{-\infty}^\infty dy\ \left(B_x{}^{\mathrm{II}}\frac{\partial B_x{}^{\mathrm{II}}}{\partial z} + B_y{}^{\mathrm{II}}\frac{\partial B_y{}^{\mathrm{II}}}{\partial z} - B_z{}^{\mathrm{II}}\frac{\partial B_z{}^{\mathrm{II}}}{\partial z}\right)\bigg|_{z=0} + \int_{-d}^0 dz\int_{-\infty}^\infty dy\left(B_x{}^{\mathrm{II}}\frac{\partial B_x{}^{\mathrm{II}}}{\partial x}\right)\bigg|_{x=0}\right] - \frac{\Phi_0}{8\pi}\int_{-d}^0 dz\, B_z{}^{\mathrm{II}}|_{|\boldsymbol{\rho}-\boldsymbol{\rho}_0|\approx\xi} = F^{(S)} + F^{(\mathrm{edge})} + F^{(\mathrm{shaft})}. \tag{16}$$

The various terms in Eq. (16) have obvious association with the surfaces of domain II, see Fig. 1(b). From the expressions in the Appendix it follows that

$$\frac{\partial B_x^{(\mathrm{II})}(\mathbf{r};x_0)}{\partial x}\bigg|_{x=0} = B_y^{(\mathrm{II})}(\mathbf{r};x_0)\bigg|_{x=0} = B_z^{(\mathrm{II})}(\mathbf{r};x_0)|_{x=0} = 0,$$

$$j_x^{(\mathrm{II})}(\mathbf{r};x_0)|_{x=0} = j_z^{(\mathrm{II})}(\mathbf{r};x_0)|_{x=0} = 0, \quad j_y^{(\mathrm{II})}(\mathbf{r};x_0)|_{x=0} \neq 0, \tag{17}$$

hence, $F^{(\mathrm{edge})}=0$ in Eq. (16). Also the integration over the shaft surface in cylindrical coordinates yields[17]

$$F^{(\mathrm{shaft})} \approx d\left(\frac{\Phi_0}{4\pi\lambda}\right)^2 \ln\left(\frac{\lambda}{\xi}\right) = F^{(\mathrm{shaft})}(d). \tag{18}$$

The free energy expression in Eq. (18) is recognized as the Abrikosov vortex intrinsic free energy, prorated to a film of thickness d. In keeping with its intrinsic character, this free energy contribution is independent of the vortex location. Thus, the entire vortex-location dependence of $F^{(\mathrm{surf})}$ is carried by the term $F^{(S)}$ in Eq. (16), associated with the top and bottom surfaces of domain II. This observation is relevant to the pinning potential calculation below.

To gain insight into the free energy film-thickness dependence consider first the infinite slab configuration of Fig. 1(a). The decomposition in Eq. (16) holds true for this configuration provided that the integration extends over the entire x axis and the $F^{(\mathrm{edge})}$ contribution is dropped. Straightforward algebra yields the closed forms,

$$F^{(\mathrm{out})}(d) = 4\pi\int_0^\infty dk_x\int_0^\infty dk_y\sqrt{k_x{}^2+k_y{}^2}\,W^2(k_x,k_y),$$

$$F^{(\mathrm{surf})}(d) = F^{(S)}(d) + F^{(\mathrm{shaft})}(d),$$

$$F^{(S)}(d) = \left(\frac{4\pi}{\gamma^2}\right)\int_0^\infty dk_x\int_0^\infty dk_y(k_x{}^2+k_y{}^2)W^2(k_x,k_y) \times\{\sqrt{k_x{}^2+k_y{}^2} + D(k_x,k_y)\coth[D(k_x,k_y)(d/2)]\}, \tag{19}$$

where the notation of the free energy terms $F^{(\mathrm{out})}(d)$, $F^{(\mathrm{surf})}\times(d)$, and $F^{(S)}(d)$ [Eq. (14)] underscore the reference to an infinite slab, where the free energy depends on the film thickness d, yet independent of the vortex location.

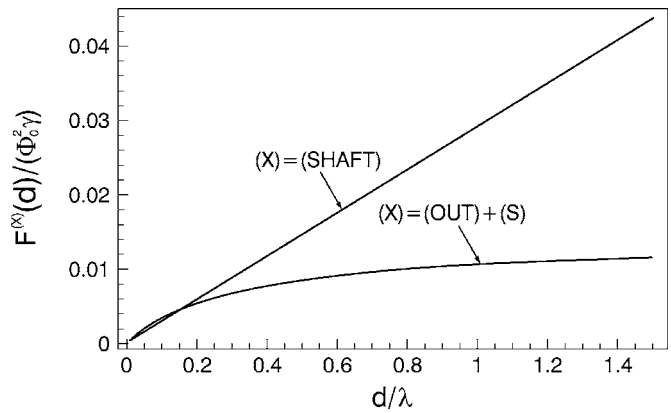

FIG. 2. The dimensionless free energy of a single vortex in an infinite finite-thickness film configuration as a function of the film thickness, Eqs. (18) and (19). The notation $F^{(\mathrm{out})+(S)}(d)$ abbreviates the sum $F^{(\mathrm{out})}(d)+F^{(S)}\times(d)$.

The film-thickness dependence of the terms in Eq. (17) is plotted in Fig. 2. The individual curves for $F^{(S)}(d)$ and $F^{(\mathrm{out})}(d)$ (not shown) are qualitatively and quantitatively similar. Note that the curve for $F^{(S)}(d)+F^{(\mathrm{out})}(d)$ saturates at $d/\lambda \geqslant 2$, unlike the vortex intrinsic free energy $F^{(\mathrm{shaft})}(d)$ which grows linearly with film thickness, Eq. (18). The saturation of $F^{(S)}(d)+F^{(\mathrm{out})}(d)$ is interpreted to indicate that these contributions originate primarily from the thickness dependence of the B_x and B_y components, see also Eq. (16). These field components are significant primarily near the top and bottom surfaces of the film. Hence, for sufficiently large film thicknesses, when the top and bottom film surfaces do not interfere with each other, these components saturate to a thickness-independent value.[7] The $F^{(\mathrm{shaft})}$ term, on the other hand, is associated primarily with the B_z component, which persists throughout the film regardless of its thickness. Mathematically, the saturation of $F^{(S)}(d)+F^{(\mathrm{out})}(d)$ terms is manifest in Eq. (19) via its $\tanh(x)$ thickness dependence [or $\coth(x)$], which saturates for $x>1$. Note from Fig. 2 that notwithstanding that the free energy contribution $F^{(\mathrm{shaft})}$ is usually the largest contribution, in the context of pinning it is irrelevant since it does not depend on the vortex location, see below.[16]

Returning to the vortex in a semi-infinite finite-thickness film configuration, Fig. 1(b). Employing Eqs. (8), (9), (A2), (15), and (16) yields

$$F^{(\mathrm{out})\mathrm{I+III}}(x_0,d) = 16\pi\int_0^\infty dk_x\int_0^\infty dk_y\sqrt{k_x{}^2+k_y{}^2} \times W^2(k_x,k_y)\sin^2(k_x x_0),$$

$$F^{(\mathrm{out})\mathrm{IV}}(x_0,d) = 8\pi\int_0^\infty dk_x\int_0^\infty dk_y \times\frac{k_x D(k_x,k_y)W^2(k_x,k_y)\sin^2(k_x x_0)}{\sqrt{k_x{}^2+\gamma^2}} \times\coth[D(k_x,k_y)(d/2)],$$

Downloaded 18 Aug 2008 to 160.91.172.37. Redistribution subject to AIP license or copyright; see http://jap.aip.org/jap/copyright.jsp

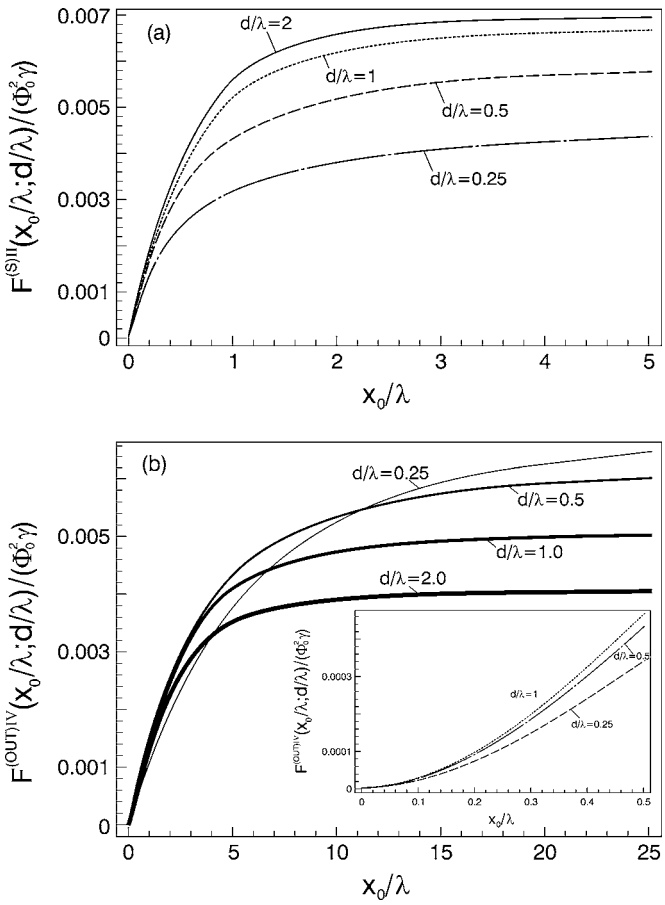

FIG. 3. The dimensionless free energy of a single vortex in a semi-infinite film as a function of the vortex location and film thickness, Eq. (20). (a) The contribution from the superconductor body of domain II in Fig. 1(b). (b) The contribution from the free space portion of domain IV in Fig. 1(b). The inset amplifies the dependencies in the $x_0/\lambda \ll 1$ domain, while the figure focuses on the $x_0/\lambda > 1$ domain.

$$F^{(S)\mathrm{II}}(x_0,d) = \left(\frac{8\pi}{\gamma^2}\right)\int_0^\infty dk_x \int_0^\infty dk_y (k_x{}^2 + k_y{}^2) W^2(k_x,k_y)\sin^2(k_x x_0) \times \{\sqrt{k_x{}^2+k_y{}^2} + D(k_x,k_y)\coth[D(k_x,k_y)(d/2)]\}, \tag{20}$$

where the domain label in each free energy term indicates the associated spatial domain. The dependence of the free energy terms in Eq. (20) on both (x_0,d) parameters is a consequence of the edge in the semi-infinite finite-thickness film. Note that in all terms in Eq. (20) the vortex location dependence enters through a $\sin^2(k_x x_0)$ factor. This factor vanishes for $x_0=0$, reflecting the fact that in this limit the vortex and antivortex pairs coalesce and cancel out each other.

The terms in Eq. (20) are plotted in Fig. 3. In Fig. 3(a) we plot $F^{(S)\mathrm{II}}(x_0,d)$, which involves the exact field components. In the limit when the vortex location is far from the film's edge, when $x_0/\lambda \gg 1$, this term should coincide with that of an infinitely extended film, Eq. (19). Indeed, noting that $\lim_{x_0\to\infty}\sin^2(k_x x_0) \approx \langle \sin^2(k_x x_0)\rangle = 0.5$, it follows that $\lim_{x_0/\lambda\to\infty} F^{(S)\mathrm{II}}(x_0,d) \approx F^{(S)}(d)$. This limiting value is realized for $x_0 = O(\lambda)$, which is manifested as the free energy saturation as a function of x_0/λ, Fig. 3(a), the same with the free energy saturation for the infinite film configuration in Fig. 2.

Consider now the free energy contribution stored in the field outside the sample. For this free energy contribution, the semi-infinite finite-thickness film and the infinitely extended film differ *qualitatively* since the field lines in the former must wrap around the film's edge. This costs extra energy, see Fig. 1(b). This interplay is represented by the $F^{(\mathrm{out})\mathrm{IV}}(x_0,d)$ term in Eq. (20) and is plotted in Fig. 3(b). When $x_0/\lambda < 1$, i.e., the vortex is near the film's edge, the free energy *increases* with d/λ for "small" d/λ since for the field lines to form closed loops threading at the vortex location implies an increase of field lines bending with increased film thickness, see inset to Fig. 3(b). On the other hand, when $x_0/\lambda \gg 1$, i.e., the vortex is far from the film's edge, for the lines to form closed loops threading at the vortex location implies that the thicker the film the lesser the field lines bending. Hence $F^{(\mathrm{out})\mathrm{IV}}(x_0,d)$ decreases with increasing film thickness, see Fig. 3(b). The energy cost associated with field line bending around the film's edge is also reflected in the term $F^{(\mathrm{out})\mathrm{I+III}}(x_0,d)$, Eq. (20). Comparison of the expressions in Eqs. (19) and (20) in the $x_0/\lambda \gg 1$ limit implies that the magnetic field energy stored in domains I+III is twice that of an infinite film. This free energy excess of the semi-infinite film (over that of an infinite film) is interpreted to be associated with field lines bending around its edge.

Having calculated the free energy dependence on the vortex location x_0, the critical current *parallel* to the film's edge is determined by equating the associated Lorentz force with the pinning force. The latter is obtained from the derivative of the free energy *per vortex unit length*.[11,16,17,19] The free energy differential resulting from the presence of an edge is [Eqs. (14)–(16)]

$$U(x_0,d) = F^{(\mathrm{surf})}(x_0,d) + F^{(\mathrm{out})}(x_0,d) - F^{(\mathrm{shaft})}(d). \tag{21}$$

Accordingly, the critical current parallel to the film's edge, denoted by $j_c(\|;d)$, is

$$j_c(\|;d) \approx \left(\frac{c}{\Phi_0}\right)\left\langle \frac{\partial}{\partial x_0}\left(\frac{U(x_0,d)}{d}\right)\right\rangle\Bigg|_{x_0=x_M}, \tag{22}$$

where the parentheses $\langle\ \rangle$ denote spatial coarse-grain averaging of the derivative and x_M denotes the "probable" location of the pinned vortex. This spatial coarse-grain derivative averaging represents an inherent uncertainty in the vortex core location due to its size and thermal agitation. We expect it to be inconsequential in our case of a considerably extended vortex. The appropriate choices of the spatial coarse-grain averaging and x_M depend on context and are discussed below.

The dimensionless quantity proportional to the free energy per vortex unit length $U(x_0,d)/d$ is plotted in Fig. 4(a). As Fig. 4(a) clearly indicates, the free energy per vortex unit length slopes increases with decreasing d/λ for all vortex location x_0. This implies that regardless of the particular choice for the derivative evaluation point x_M in Eq. (22), the calculated critical current given by Eq. (22) increases with decreasing d/λ. This trend is the same with that observed for

Downloaded 18 Aug 2008 to 160.91.172.37. Redistribution subject to AIP license or copyright; see http://jap.aip.org/jap/copyright.jsp

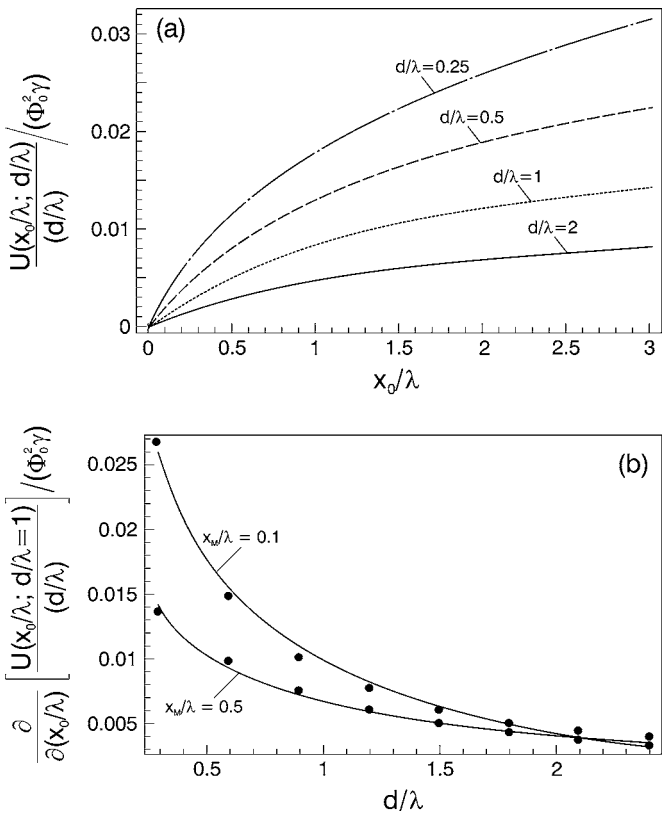

FIG. 4. The dimensionless pinning potential and pinning force per vortex unit length. (a) The dimensionless pinning potential per vortex unit length. Note that the slope saturation is denoted as $d/\lambda \geqslant 2$. (b) The dimensionless pinning potential per vortex unit length coarse-grain averaged derivative as a function of the film thickness for two choices of the evaluation point x_M/λ. The dots denote the calculated derivative at selected points while the solid line is a fit to the two-parameter expression $a+b/\sqrt{(d/\lambda)}$. For the $x_M/\lambda=0.1$ curve, the best-fit parameters are $a=-0.0094$ and $b=0.0195$, and for the $x_M/\lambda=0.5$ curve the best-fit parameters are $a=-0.0016$ and $b=0.0095$.

critical currents in thin films, such as epitaxial films and porous and nonporous CCs.[1–4] Another interesting feature exhibited in Fig. 4(a) is that the slope itself tends toward saturation as $d/\lambda \to 2$ (curves corresponding to higher d/λ values are not plotted). A similar type of saturation has been observed in some of the data.[3]

Consider Fig. 4(b), it shows the dimensionless quantity corresponding to the averaged free energy derivative, [Eq. (22)] for two rather different choices of the probable location of the pinned vortex x_M. The $\langle \cdots \rangle$ brackets in the ordinate of Fig. 4(b) are omitted to simplify the notation. The derivative is spatially coarse-grain averaged over an interval $\Delta x_0/\lambda=0.1$, which is a high multiple of the vortex's core size. As mentioned above, the particular choice of x_M in Eq. (22) depends on context. For example, in the context of a low-angle grain boundary, modeled as a periodic array of dislocations or as a thin degraded superconductor buffer layer, the probable vortex location is at or around the grain boundary plane.[11,15,18] In this case $x_M=O(\xi)$, where ξ denotes the coherence length. On the other hand, in the context of porous superconductor films one may argue that the flux is being pinned against entry into the superconductor film, which implies a choice $x_M<\lambda$. The point of Fig. 4(b) is to demonstrate that the calculated critical current film-thickness scaling law is insensitive to the particular choice of $x_M<\lambda$, i.e., it has the form $j_c(\|;d) \propto a+b/\sqrt{d}$; the constants a and b quoted in the figure caption depend on the particular choice of x_M. This type of film-thickness scaling law is consistent with that observed in CC.[1–3]

It is instructive to estimate the calculated critical currents from Eq. (22). For the parameters $x_M/\lambda=0.1$ and film thickness $d/\lambda=1$ the calculated dimensionless derivative from Fig. 4(b) is ≈ 0.012. Inserting it in Eq. (22) together with the YBCO penetration depth value $\lambda(T=77\text{ K})=310$ nm and the constants $\Phi_0=1630\text{ eV D}^{1/2}$, $1\text{ A/cm}^2=2381\text{ eV}^{1/2}/(\text{s D}^{3/2})$ yields

$$j_c(\|;d/\lambda=1) \approx \frac{\Phi_0 c}{\lambda^3}\left\langle \frac{\partial}{\partial(x_0/\lambda)}\left(\frac{\lambda}{d}\right) \times \left(\frac{U(x_0/\lambda;d/\lambda=1)}{\Phi_0^2\gamma}\right)\right\rangle\Bigg|_{x_0/\lambda=x_M/\lambda=0.1} \approx 0.82\text{ MA/cm}^2 \tag{23}$$

This parameter-free calculated value is within a factor of 3 of measured values in CC at this particular film thickness.[2]

The results in Fig. 4(b) and Eq. (23) for the semi-infinite finite-thickness film configuration investigated here raise the question of their relevance in the more general context of critical currents in thin superconductor films, e.g., porous films on vicinal substrates,[10] epitaxial thin films, and CC.[1–4] As mentioned above in the context of porous films, the present model represents an idealization of the pore edges and their pinning properties against flux penetration into the film. In the context of twin boundary models, sometimes modeled as a thin buffer layer separating two massive superconductors,[16,20] the present configuration represents one bank of that configuration. While the following is not intended as a proof, it is expected that the film-thickness dependence in these cases will be similar to that calculated here since, as argued here, it is the vortex structure that invokes the film thickness dependence. In the context of realistic low-angle grain boundary models[11,19,21] the situation is not clear and further studies are called for.

In summary, we examined the configuration of a semi-infinite finite-thickness film in the presence of a single vortex, in order to explore the film-thickness dependence in the simple case of pinning by a single surface and the associated critical current film-thickness dependence. The calculated critical current scales with film thickness as $a+b/\sqrt{d}$, where a and b are constants, and implies saturation of the film-thickness dependence at and beyond $d/\lambda \approx 2$. Furthermore, the parameter-free calculated critical current for a "typical" film thickness $d/\lambda=1$ falls within less than a factor of 3 of that observed values in CC. Although we make no claim that this configuration is realistic, it nevertheless embodies some of the characteristics of common defects in YBCO thin films such as grain and twin boundaries, pores and inclusions, and vortex broadening. While the similarities of our results to the observed film thickness scaling in porous films[10] and CC Refs. [2–4] are no proof of its general applicability, they are encouraging and raise the possibility that some of the observed film thickness dependence is of geometrical origin.

Downloaded 18 Aug 2008 to 160.91.172.37. Redistribution subject to AIP license or copyright; see http://jap.aip.org/jap/copyright.jsp

ACKNOWLEDGMENTS

This research is sponsored by Oak Ridge National Laboratory, managed by UT-Battelle, LLC for the United States Department of Energy under Contract No. DE-AC05-00OR22725. One of the authors (D.A.) would like to thank the Naval Surface Warfare Center, ILIR program, and the Oak Ridge National Laboratory for the support.

APPENDIX: VORTEX STRUCTURE IN A FINITE-THICKNESS SEMI-INFINITE SUPERCONDUCTING FILM

Consider the exact solution in domain II, i.e.,

$$\mathbf{B}^{\mathrm{II}}(\mathbf{r};x_0) = \mathbf{B}^{(\mathrm{V})\mathrm{II+IV}}(\mathbf{r};x_0) - \mathbf{B}^{(\mathrm{V})\mathrm{II+IV}}(\mathbf{r};-x_0),$$

based on the explicit expressions of the vortex structure in an infinite film, Eqs. (4) and (6), it follows immediately that

$$B_{x,y}{}^{\mathrm{II}}(\mathbf{r};x_0) = \int_{-\infty}^{\infty} dk_x \int_{-\infty}^{\infty} dk_y e^{i(k_x x + k_y y)} \times \frac{\sinh[D(k_x,k_y)(z+d/2)]}{\sinh[D(k_x,k_y)(d/2)]} \alpha_{x,y}{}^{\mathrm{II}}(x_0),$$

$$B_z{}^{\mathrm{II}}(\mathbf{r};x_0) = \int_{-\infty}^{\infty} dk_x \int_{-\infty}^{\infty} dk_y e^{i(k_x x + k_y y)} \times \frac{\cosh[D(k_x,k_y)(z+d/2)]}{\cosh[D(k_x,k_y)(d/2)]} \alpha_z{}^{\mathrm{II}}(x_0), \qquad \text{(A1)}$$

where

$$\alpha_x{}^{\mathrm{II}}(x_0) = -2k_x W(k_x,k_y)\sin(k_x x_0),$$

$$\alpha_y{}^{\mathrm{II}}(x_0) = -2k_y W(k_x,k_y)\sin(k_x x_0),$$

$$\alpha_z{}^{\mathrm{II}}(x_0) = i\frac{2(k_x{}^2 + k_y{}^2)W(k_x,k_y)\sin(k_x x_0)}{D(k_x,k_y)\tanh[D(k_x,k_y)(d/2)]} - i\frac{\gamma^2\Phi_0 \sin(k_x x_0)}{2\pi^2 D(k_x,k_y)^2}. \qquad \text{(A2)}$$

[1] W. V. Hassenzahl, D. W. Hazelton, B. K. Johnson, P. Komarek, M. Noe, and C. T. Reis, Proc. IEEE **92**, 1655 (2004).
[2] A. O. Ijaduola, J. R. Thompson, R. Feenstra, D. K. Christen, A. A. Gapud, and X. Song, Phys. Rev. B **73**, 134502 (2006); R. Feenstra, A. A. Gapud, F. A. List, E. D. Specht, D. K. Christen, T. G. Holesinger, and D. M. Feldman, IEEE Trans. Appl. Supercond. **15**, 2803 (2005); T. G. Holesinger, P. N. Arendt, R. Feenstra, A. A. Gapud, E. D. Specht, D. M. Feldman, and D. C. Larbaletier, J. Mater. Res. **20**, 1216 (2005).
[3] S. R. Foltyn, H. Wang, L. Civale, Q. X. Jia, P. N. Arendt, B. Maiorov, Y. Li, M. P. Maley, and J. L. MacManus-Driscoll, Appl. Phys. Lett. **87**, 162505 (2005); S. R. Foltyn *et al.*, Appl. Phys. Lett. **82**, 4519 (2003); Q. X. Jia, S. R. Foltyn, P. N. Arendt, and J. F. Smith, Appl. Phys. Lett. **80**, 1601 (2002); S. R. Foltyn, Q. X. Jia, P. N. Arendt, Y. Fan, and J. F. Smith, Appl. Phys. Lett. **75**, 3692 (1999).
[4] S. R. Foltyn, P. Tiwari, R. C. Dye, M. Le, and X. D. Wu, Appl. Phys. Lett. **63**, 1848 (1993).
[5] S. I. Kim, A. Gurevich, X. Song, X. Li, W. Zhang, T. Kodenkandath, M. W. Rupich, T. G. Holesinger, and D. C. Larbalestier, Supercond. Sci. Technol. **19**, 968 (2006).
[6] A. Larkin and Yu. Ovchinnikov, J. Low Temp. Phys. **34**, 409 (1979); G. Blatter, M. Feigelman, V. M. Geshkenbein, and V. M. Vinokur, Rev. Mod. Phys. **66**, 1125 (1994).
[7] D. Agassi and J. R. Cullen, Physica C **334**, 274 (2000).
[8] J. Pearl, Appl. Phys. Lett. **5**, 65 (1964).
[9] A. A. Abrikosov, *Fundamentals of the Theory of Metals* (North-Holland, Amsterdam, 1988), Sec. 18.5.
[10] R. L. S. Emergo, J. Z. Wu, T. J. Haugan, and P. N. Barnes, Appl. Phys. Lett. **87**, 1 (2005); R. L. S. Emergo, J. Z. Wu, T. Aytug, and D. K. Christen, Appl. Phys. Lett. **85**, 618 (2004).
[11] D. Agassi, D. K. Christen, and S. J. Pennycook, Appl. Phys. Lett. **81**, 2803 (2002).
[12] A. A. Abrikosov, *Fundamentals of the Theory of Metals* (North-Holland, Amsterdam, 1988), p. 439.
[13] D. Agassi and J. J. Cullen, Physica C **323**, 94 (1999).
[14] For example, E. H. Brandt, Phys. Rev. B **64**, 024505 (2001) and references therein; E. H. Brandt, Phys. Rev. B **60**, 11939 (1999); E. H. Brandt, Phys. Rev. B **71**, 014521 (2005).
[15] P. M. Morse and H. Feshbach, *Methods of Theoretical Physics* (McGraw-Hill, New York, 1953), pp. 808–816.
[16] D. Agassi and J. J. Cullen, Physica C **195**, 277 (1992); A. M. Grishin, Sov. J. Low Temp. Phys. **9**, 138 (1983).
[17] D. Agassi and J. R. Cullen, Physica C **316**, 1 (1999).
[18] J. D. Jackson, *Classical Electrodynamics*, 2nd ed. (Wiley, New York, 1975), Sec. 1.4; H. P. Neff, Jr., *Basic Electromagnetic Fields* (Harper & Row, New York, 1981), p. 567.
[19] D. Agassi, C. S. Pande, and R. A. Masumura, Phys. Rev. B **52**, 16237 (1995).
[20] I. Maggio April, Ch. Renner, A. Erb, E. Walker, and O. Fischer, Nature (London) **390**, 487 (1997).
[21] A. Gurevich and E. A. Pashitskii, Phys. Rev. B **57**, 13878 (1998).

Downloaded 18 Aug 2008 to 160.91.172.37. Redistribution subject to AIP license or copyright; see http://jap.aip.org/jap/copyright.jsp